33p

NASA TN D-1826

TECHNICAL NOTE

D-1826

PRELIMINARY FLIGHT EVALUATION

OF TWO UNPOWERED MANNED PARAGLIDERS

By Garrison P. Layton, Jr., and Milton O. Thompson

Flight Research Center
Edwards, Calif.

NATIONAL AERONAUTICS AND SPACE ADMINISTRATION

WASHINGTON

April 1963

NATIONAL AERONAUTICS AND SPACE ADMINISTRATION

TECHNICAL NOTE D-1826

PRELIMINARY FLIGHT EVALUATION OF TWO UNPOWERED MANNED PARAGLIDERS

By Garrison P. Layton, Jr., and Milton O. Thompson

SUMMARY

Towed and free-flight tests were made with unpowered, manned paragliders to study the performance, stability, and control characteristics of a typical paraglider. The paragliders used had maximum lift-drag ratios greater than 3.5 and wing loadings of approximately 4.0 lb/sq ft. The airspeed range was limited by the rearward center-of-pressure shift at angles of attack above and below trim angle of attack. Performance data obtained from flight tests are presented and compared with analytical results. Center-of-gravity shift, accomplished by tilting the wing relative to the fuselage, was used for control. This method of control was adequate for towed and free flight as well as for flare and landing. The pilot's evaluation of the vehicle's handling qualities, and a discussion of development problems are presented.

INTRODUCTION

Paragliders have been proposed for use in the recovery of space vehicles (ref. 1, for example) and for other purposes such as logistics support vehicles and booster recovery vehicles. Paragliders have two significant advantages over other vehicles proposed for these applications. They can be maneuvered to a predetermined landing point and can be landed with near-zero vertical velocity.

To complement wind-tunnel tests and flight tests of paragliders by other facilities (refs. 2 and 3), the NASA Flight Research Center at Edwards, Calif., built and is flying two manned unpowered paragliders. The objective of the program is to achieve manned, controlled free glide flight and to demonstrate the flare and landing capability of a paraglider with a maximum lift-drag ratio less than 3.0 and a wing loading up to 7.0 lb/sq ft.

This paper presents some of the initial results of this investigation in which, for safety reasons, maximum lift-drag ratios greater than 3.5 and wing loadings of approximately 4.0 lb/sq ft were used.

SYMBOLS

All forces and moments are presented with respect to a system of body axes originating at the intersection of the centerlines of the booms and the keel. Coefficients are based on the wing membrane area and the keel length.

a_n	normal acceleration, g units
C_D	drag coefficient, $\frac{\text{Drag}}{qS}$
C_L	lift coefficient, $\frac{\text{Lift}}{qS}$
C_m	pitching-moment coefficient, $\frac{\text{Pitching moment}}{qSl_k}$
C_{m_α}	slope of pitching-moment curve, $\frac{\partial C_m}{\partial \alpha}$, per deg
C_N	normal-force coefficient, $\frac{\text{Normal force}}{qS}$
C_{N_α}	slope of normal-force curve, $\frac{\partial C_N}{\partial \alpha}$, per deg
C_X	chordwise force coefficient, $\frac{\text{Chordwise force}}{qS}$
C_{X_α}	slope of chordwise force curve, $\frac{\partial C_X}{\partial \alpha}$, per deg
D	drag, lb
g	acceleration due to gravity, ft/sec^2
i	wing incidence angle, deg
L	lift, lb
ΔL	incremental lift due to gust
l_k	keel length, ft
q	dynamic pressure, lb/sq ft
S	wing area (based on flat planform), sq ft
V	free-stream velocity, knots
ΔV	gust velocity, knots

V_0	free-stream velocity prior to gust, ft/sec
V_v	vertical velocity, ft/sec
W	weight, lb
X,Z	body reference axes
x	distance along X-axis, positive rearward along the keel, ft
z	distance along Z-axis, positive downward perpendicular to the keel, ft
x_0, z_0	position of aerodynamic center, ft
α	angle of attack, deg
γ	glide-path angle, deg
δ	angular position of aircraft center of gravity with respect to a line perpendicular to the wing through the aerodynamic center, deg
θ	pitch attitude, deg
ρ	mass density of air (0.00224 used for all theoretical calculations), slugs/cu ft

Subscript:

w	wing

DESCRIPTION OF THE TEST VEHICLES

Photographs showing details of vehicle A and vehicle B are presented in figures 1 and 2, respectively. Figures 3 and 4 are three-view drawings of the vehicles. Pertinent physical characteristics are presented in table I.

The fuselages of both vehicles were constructed of steel tubing and were of the open-framework type. The keel and leading edges of the wings were constructed of 2 1/2-inch-diameter aluminum tubing. The boom sweep angle was held constant at 50° by the use of a rigid spreader bar. Additional wing structure fabricated of steel tubing assured structural integrity.

The pilot's display consisted of rate-of-climb, altitude, and airspeed indicators. Fuselage pitch attitude and wing incidence angle were presented for data purposes.

The principal differences between the two vehicles are shown in the following table:

Component	Vehicle A	Vehicle B
Fuselage	Main longitudinal member was single 1 1/2-inch-diameter tube (fig. 1)	Built-up truss, instead of single tube (fig. 2)
Control system	Direct link (fig. 5)	Cable-operated (fig. 6)
Wing membrane	Doped Irish linen	6-ounce unsealed Dacron (fig. 7)
Main landing gear	Single steel tube (fig. 1)	Shocks and bungees used (fig. 2)

TEST TECHNIQUES

The paragliders were towed aloft during all flight tests. The first tests were conducted with a truck as the tow vehicle (ground tow). Later tests used a light aircraft to tow the paragliders (air tow).

Ground Tow

Initial tests with each vehicle were made with a 300-foot towline at speeds near the speed for nosewheel lift-off. The pilot evaluated the control effectiveness both laterally and longitudinally during these tests. When the pilot felt that control was adequate, speed was increased until lift-off occurred. The pilot then further evaluated the control, with particular attention to the control forces. The distance between the pivot point and the wing center of pressure of a paraglider determines the stick forces. The sail position relative to the pivot point was changed between flights of the test vehicles until the trim stick forces were acceptable near the airspeed for maximum lift-drag ratio.

A 1,000-foot towline was used for subsequent tows to obtain altitudes of 200 feet, from which stabilized glides and complete flares and landings were accomplished.

A Fairchild multiple-exposure theodolite camera was used to obtain all quantitative data from ground tows. The basic data obtained with this technique were the variation of range, altitude, and pitch attitude with time (fig. 8). From these data, vertical velocity, horizontal velocity, flight-path angle, angle of attack, and lift-drag ratio were determined. The Fairchild data were used primarily to evaluate the flare and landing. Since a steady-state glide could be maintained for only 1 second to 1.5 seconds, only approximate values of lift-drag ratio were obtained.

Air Tow

During all air tows, a 1,000-foot towline was used to keep the paraglider out of the wake of the tow airplane and to provide a minimum angular deflection from the flight path.

Before data were obtained on free flights from air tow, the airspeed indicator was calibrated by checking it against the tow truck's calibrated speedometer during ground tow.

During free flights from air tow, performance data, the only quantitative data obtained, were derived by recording the time required to descend 2,000 feet at a constant airspeed. The pilot recorded fuselage attitude and wing incidence during these stabilized glides to determine angle of attack. The air-tow data flights were conducted only when winds were calm to assure repeatability of data.

RESULTS AND DISCUSSION

The initial design of the Flight Research Center paragliders was based on the results of wind-tunnel and free-flight model tests. Simplicity of construction, economy, ease of maintenance and modification, and construction time were also important considerations. Expeditious program progress was mandatory if the flight-test results were to be of significant value in the design of operational systems utilizing the parawing concept. Pilot-safety considerations were, however, the controlling factor in actual operation. The vehicles shown in figures 1 and 2 were the products of these considerations. Modifications to the initial configuration were incorporated only as necessary to accomplish the initial test objective or to satisfy piloting considerations.

Performance Data

Vehicle A.- The maximum lift-drag ratio for vehicle A was 3.5 at 42 knots, instead of the predicted value of 4.2 (fig. 9). The minimum rate of sink was 17 ft/sec at 35 knots, instead of the predicted minimum rate of sink of 15 ft/sec (fig. 10). There are two reasons for this variation. First, the membrane shape was poor, with large spanwise seams and a fluttering trailing edge. Second, the vehicle employed considerably more structure than was accounted for in the original drag analysis.

Vehicle B.- Performance data obtained during sustained free flight show that the maximum lift-drag ratio for vehicle B was 3.9 at 42 knots instead of the predicted 3.1 (fig. 11), with a corresponding decrease to 16.5 ft/sec in minimum vertical velocity (fig. 12).

Handling Qualities

The stability and control characteristics of the paraglider configurations tested were adequate to accomplish the primary objectives of a paraglider

recovery system, that is, to land at a designated area with near-zero vertical velocity. Atmospheric conditions during the test program, however, were a controlling factor in scheduling flights. Steady winds in excess of 12 knots, horizontal gusts in excess of ±5 knots, and moderate turbulence, either combined or separately, constituted "no flight" conditions.

Basic static stability and handling-qualities characteristics of a parawing-payload combination are dependent upon the selection and use of various physical and aerodynamic relationships. These characteristics, which were obtained from wind-tunnel tests of various wings and wing-payload combinations, are included in the appendix for the paragliders used in the Flight Research Center program. Flight-test results indicate good agreement in these areas. Dynamic stability and control characteristics are not as readily available as static characteristics, since data from manned paraglider flight experience are extremely limited. No standards exist, and present standards for flight vehicles are not directly applicable. The discussion in this section is devoted primarily to vehicle characteristics observed as a result of maneuvering flight.

The selection of a universal pivot for the wing, located near the wing center of pressure, was responsible for certain characteristics of the Flight Research Center paraglider which are not common to a vehicle utilizing cable-sling connections between the wing and payload. Stick-free vehicle stability of the test vehicles was equivalent to the stability of the wing about the pivot and did not include the increment of stability resulting from the low center-of-gravity position.

The basic vehicle geometry and physical characteristics of the test vehicles were responsible for some unusual vehicle responses to applied control and gust forces. Four conditions determined the type of vehicle response: (1) the type of control utilized, for example, center-of-gravity shift; (2) the combined lateral-directional characteristics of the isolated wing; (3) the nonrigid wing-payload attachment; and (4) the displacement of the pilot from the pitch and roll axes. The unusual motion cues noted at the pilot's station as a result of control application sometimes resulted in reversed pilot inputs or hesitancy in completion of a control application. The initial fuselage motion was in the opposite direction from that of the intended and ensuing maneuver. This center-of-gravity-shift type of control was responsible for some undesirable handling qualities. The high inertias, moderate friction, and large deflections required to obtain a rapid vehicle attitude change were characteristics which reduced the pilot's capability to cope with low-amplitude, short-period oscillations, and increased the probability of augmenting rather than damping a motion. As a result, the pilot relied on the inherent vehicle stability, both dynamically and statically, and used small-amplitude, long-duration control inputs to produce vehicle attitude changes. The center-of-gravity shift produced low initial accelerations, but was effective and capable of high rates with prolonged application of even small control deflections.

Longitudinal handling qualities.- Vehicle response to step longitudinal control inputs consisted of an initial motion of the lower fuselage about the pivot point which resulted in a wing-incidence change and a total vehicle attitude change. Since the pilot's normal forward field of view did not include an portion of the wing, the change in wing position relative to the lower fuselage

was not noted. The seemingly "wrong" first motion response to rapid control inputs was noted at the pilot's station, even though the change in fuselage pitch attitude was small and no visual pitch reference was available to the pilot. With slow-rate control inputs, the first motion was imperceptible, and the response was noted only as a lag from control input to vehicle attitude change. Vehicle response to gust forces was conventional in the longitudinal mode with the stick fixed, and was opposite to the response with the stick free. With the stick free, however, the rather rapid lower-fuselage motions were somewhat confusing to the pilot.

Pitching oscillations were not apparent as a result of small pulse or step type of control inputs. The only pitching oscillations noted occurred in conjunction with the higher-amplitude lateral-directional motions initiated by moderate turbulence. The pitching oscillations damped completely as the lateral-directional oscillations diminished in amplitude.

Since both of the control systems (cable and linkage) utilized in the paraglider were of a direct manual type, control forces were determined by the relationship of the wing center of pressure and the wing-pivot point, and by the selected control-system gearing. Center-of-pressure position of the initial wing was assumed to be at a 46-percent-keel location, based on reference 2. Initial flight tests revealed that extremely high (two-handed) pull forces were necessary to maintain stick position in towed flight, with only a slight reduction of these forces in free flight. Calculations using estimated values of stick force indicated that the actual center-of-pressure position was at a 47.5-percent-keel location. Relocating the wing by trial and error reduced the control forces to acceptable levels over the limited speed range of 30 KIAS to 65 KIAS.

Locating the wing so that the wing center of pressure and wing pivot point coincided was not considered desirable by the pilot. A wing position was selected, therefore, which resulted in small pull forces. The pilot's desire for a slight pull force is probably related to the fundamental difference between stick-fixed and stick-free stability. With zero stick force, the pilot would have a tendency to allow the vehicle to fly itself. The flight behavior would then be related to stick-free stability, which is equivalent to the stability of the wing about the pivot and does not include the increment of stability resulting from the low center-of-gravity position.

As the flight program progressed, changes in stick force were noted. Comparison of force levels from several flights at the same flight conditions indicated a change in position of the wing center of pressure.

As a result of the difference between the actual and the assumed center-of-pressure position and the subsequent changes observed, it was concluded that the center-of-pressure position of a lifting surface employing a flexible material is critically dependent on trailing-edge conditions, canopy-attachment details, and material deformations due either to flight loads or manufacturing flaws. During a series of flights performed within 4 hours, the control forces changed considerably as a result of stretching of the wing material.

The center of pressure of the wing may be adjusted by use of boltrope, which is, effectively, cambering of the membrane that results in a rearward center-of-

pressure shift. Boltrope ground-adjustment provisions for each of the test vehicles consisted of a continuous line through the trailing-edge seam of both lobes, which insured symmetrical adjustment.

An asymmetric boltrope adjustment (1-percent difference) was unintentionally made prior to an air-tow flight. During towed flight, a slight out-of-trim condition was noted in roll. After towline release, approximately one-half of the available lateral control was required to maintain zero roll rate.

The trend of longitudinal control forces is shown plotted against airspeed in figure 13. As airspeed was decreased from the trim speed, the wing center of pressure moved rearward, which resulted in a stable force gradient with increase in angle of attack. An increase in airspeed above the trim airspeed also caused a rearward shift of wing center of pressure, but at a greater rate. This shift resulted in an unstable force gradient at low angles of attack. The stick-force buildup in this region was abrupt and reached a magnitude in excess of an estimated 100 pounds within 20 knots to 25 knots of trim speed. Trim airspeed forces were adjusted to approximately zero, and bungees were added to increase the airspeed operating range with tolerable maximum stick forces. Because of the rate of center-of-pressure shift with increasing airspeed, however, an increase of only 5 knots to 10 knots in usable airspeed could be obtained. A control-system stop was installed to insure that control forces could not exceed 150 pounds, thus establishing an operating limit for the vehicle. The forces indicated in figure 13 are static forces for 1 g flight conditions. Dynamic control forces further degraded the control system because of the high inertias inherent in a center-of-gravity-shift control system. These inertia forces were only apparent, however, when abrupt or large-deflection control inputs were made.

Lateral-directional handling qualities.- The basic vehicle geometry and physical characteristics of the test vehicles were responsible for some unusual lateral-directional responses to applied internal and external forces. The motions described in this section are those noted at the pilot's station and were primarily about the wing pivot point. No freedom of rotation of the wing relative to the fuselage was provided in the yaw axis; however, because of the flexibility of the tower structure and small clearances in the universal fitting, displacements in yaw of approximately 5° between the lower fuselage and the wing keel were observed.

As a result of the type of control system used, the lateral-directional modes could not be evaluated separately. Hence, a disturbance caused by either external or internal stimuli resulted in a coupled motion.

Total vehicle response to lateral-control inputs consisted of an initial lateral rotation of the lower fuselage around the wing pivot point, with a slightly delayed wing rotation laterally and directionally. This wing motion was followed by a fuselage realinement to effect equilibrium as a result of the new relationship of center of pressure and center of gravity.

Vehicle responses to external forces such as turbulence and towline dynamics were opposite to those resulting from control inputs and were disturbing to the pilot. Slight changes in the alinement or location of the lift vector resulted

in appreciable directional fuselage motions about the wing pivot point. Thus, it was concluded that a high value of directional stability existed. Lateral-directional oscillations resulting from lateral-control inputs were of small amplitude and were lightly damped.

Landing Flare and Touchdown

One of the advantages of a paraglider over a conventional parachute recovery system is the ability to achieve zero vertical velocity at touchdown by means of a flare. A primary purpose of the Flight Research Center paraglider program is to investigate the pilot's ability to accomplish this manually, or to determine the amount of assistance necessary for repeated successful landings.

Landing from ground tow.- During the early phases of the flight program, numerous landings were made with the paraglider still attached to the towline. This technique was used to familiarize the pilot with the available control responses. This method also eliminated any requirement for control corrections to compensate for transients initiated by towline release and prevented excessive directional divergences at touchdown. As confidence was established in the pilot's ability to adequately judge rate of control input required as a function of airspeed, landing flares were initiated from low altitudes (10 to 20 ft) with slack towlines. Towline slack was obtained by abruptly slowing the tow vehicle on command of the paraglider pilot. Following a series of successful landings using this technique, towline releases were made at altitudes of 10 feet to 20 feet. This procedure resulted in a wide variation of touchdown conditions, since, in less than 2 to 3 seconds, the pilot had to correct for any transients due to towline release, push over to minimize deceleration, and initiate and perform the flare. Release altitudes below 100 feet were not considered desirable, inasmuch as there was insufficient time to accomplish a proper transition from towed to free flight. Release altitudes were increased to a minimum of 200 feet for subsequent landing attempts.

During this phase of the landing investigation, flares were initiated from equilibrium-glide conditions at airspeeds between 35 knots and 60 knots. It was quickly established that flares initiated at or below 42 knots (indicated air speed for maximum lift-drag ratio) resulted in relatively high touchdown vertical velocities, with considerable variation in successive attempts. The energy available for flaring from 42 knots appeared to be an absolute minimum to achieve zero vertical velocity. Consequently, any variation in altitude of initiation or rate of control application during flare resulted in either completing the flare at or above the ground, or not completing it prior to touchdown. The energy available at airspeeds lower than 42 knots is only sufficient to reduce the equilibrium-glide vertical velocity to some minimum value greater than zero, and from 35 knots is only adequate to achieve a minimum of 8 ft/sec to 10 ft/sec. Variations in flare-initiation altitude and control rate result in even higher minimum vertical velocities. As airspeed for flare initiation is increased above 42 knots, landing can be consistently accomplished with touchdown vertical velocities of 5 ft/sec or less. This excess energy provides a slight amount of additional time from flare initiation to touchdown and also enables the pilot to make minor adjustments during the flare to compensate for errors in judging proper

flare-initiation altitude. Preflare airspeeds of 55 knots to 60 knots provided enough energy to complete an initial flare and an adjustment after flare or to vary the rate of flare to insure that zero vertical velocity was achieved at or just above the ground. The paraglider pilots considered this second technique (varying the rate of flare) to be the most desirable and utilized it for all subsequent landings. The technique allowed several longitudinal-control inputs to be made to evaluate vehicle response before reaching the minimum altitude required for completion of a flare. By this means, the rate of flare required to achieve satisfactory touchdown conditions could be continually evaluated by the pilot throughout the flare as control was applied.

The time from flare initiation to touchdown, even at the higher airspeeds, was of the order of 3 seconds to 3.5 seconds. This time is considerably less than that available to the pilot of the X-15 or similar low-lift-drag-ratio vehicles (approximately 30 seconds for the X-15), since the total energy available for flare is a function of the velocity squared.

Sixty-five landings of the test vehicles were made from equilibrium free-flight conditions by four different pilots. Only the project pilot attempted flares at airspeeds lower than 45 knots. All of the landings made from preflare airspeeds greater than 45 knots had estimated touchdown vertical velocities of 5 ft/sec or less.

All of the paraglider landings from stabilized free-flight conditions were made on Rogers Dry Lake, at Edwards, Calif. No height cues are available other than surface texture or, in some areas, marked runway lines. Reference to the barometric altimeter was by individual pilot preference; however, none of the pilots used the altimeter below 100 feet. Flare-initiation altitude was of little interest to the pilot, since flare was initiated and adjusted as a function of the pilot's capability to visually perceive closing rate with the touchdown point. This method has proved to be adequate at vertical velocities up to 35 ft/sec prior to flare. Ground effect was not apparent to the pilot during any of the flares.

Free glide and landing from air tow.- Several flights were made with release altitudes in excess of 2,000 feet above the lakebed to evaluate the capability of landing on a preselected point and heading. Geographical position at release was within 1,000 feet, horizontally, of the desired touchdown point. Approach patterns consisted of a combination of 360° turns and S-turns, with airspeed varying between 45 knots and 60 knots. The third attempt resulted in a landing within 20 feet of the desired point, and maximum deviation on subsequent landings was approximately 200 feet. These approaches were made in relatively calm conditions (light turbulence and wind velocity less than 10 knots). Familiarization and practice could reduce the dispersion on touchdown even further and, thus, could give consistent results within ±200 feet of the desired touchdown point.

CONCLUSIONS

Results of flight tests of the performance, stability, and control characteristics of two unpowered, manned paragliders led to the following conclusions:

1. Using a center-of-gravity-shift control system, a vehicle of this type can be controlled in towed flight, free flight, and flare and landing.

2. The available airspeed range of 30 KIAS to 65 KIAS was limited by the rearward center-of-pressure shift at angles of attack above and below trim angle of attack.

3. A vehicle of this type can be maneuvered to a predetermined landing point.

4. The landing flare must be initiated at a speed higher than that required for minimum steady-state flight-path angle to consistently achieve acceptable vertical velocities at touchdown in the short time (2 to 3 seconds) available for flare.

5. Wind-tunnel tests may be inadequate to determine the center of pressure of a paraglider because of small differences in membrane shape. This is also true for flight wings; each wing must be trimmed individually or provisions must be made in the control system to account for center-of-pressure shifts caused by small differences in membrane shape.

Flight Research Center,
National Aeronautics and Space Administration,
Edwards, Calif., February 6, 1963.

APPENDIX

ANALYSIS OF PARAGLIDER AERODYNAMICS

Performance

Wind-tunnel data (ref. 2) from a wing geometrically similar to the wings of the test vehicles and the estimated drag of the fuselage were used to determine the lift-drag characteristics and steady-state flight conditions of the vehicles.

The fuselage drag of vehicle A was estimated by considering the drag of each of the following components, assuming no interference effects: pilot, 30 feet of 1 1/2-inch-diameter tubing perpendicular to the airstream (supercritical Reynolds number), wheels, and instrument panel (ref. 4). The summation of the drag of these components yields a total drag coefficient of the fuselage of 0.06, based on the wing area. This fuselage drag was summed with the wing data to obtain the lift-drag-ratio and steady-state flight data presented in figures 9 and 10.

The lift-drag characteristics of vehicle B were estimated in a similar manner, with a more conservative estimate of the drag of the structure than was used for vehicle A. The flight data from vehicle A were also used in the analysis, inasmuch as the wing used on vehicle A was geometrically similar to the wing of vehicle B. These data were conservative, since the shape of the wing membrane on vehicle A resulted in a higher drag for the wing. The summation of the drag of the components of the fuselage yields a total drag coefficient of the fuselage of 0.123, based on the wing area. This fuselage drag summed with the wing drag yields the lift-drag characteristics and steady-state flight conditions of vehicle B presented in figures 11 and 12.

Gust Effects

Vehicles with low wing loadings are particularly susceptible to gusts. To determine the effect of gusts on the test vehicles, the initial normal acceleration resulting from a 5-knot gust was calculated. The analysis of this condition is based on the following assumptions: gust acts as a pure step in horizontal velocity, only initial accelerations are considered, and the lift coefficient is constant. Considering these assumptions, the initial normal accelerations from a 5-knot gust were calculated from the equation

$$a_n = \frac{\Delta L}{W} = \frac{C_L}{2W}\rho S\left[\left(\frac{V_0}{0.594} + \frac{\Delta V}{0.594}\right)^2 - \left(\frac{V_0}{0.594}\right)^2\right] \qquad (1)$$

and are presented in figure 14 as a function of C_L. This acceleration disturbed the vehicle from the flight path and was critical during the flare maneuver since the vehicle did not have adequate lift-drag ratio to recover.

Longitudinal Stability and Control

The following longitudinal stability and control analysis was performed to determine the range of center-of-gravity travel required and to determine that the stability was adequate over this range for the test vehicles. In this analysis, the following assumptions were made: an aerodynamic center does exist, C_{N_α} and C_{X_α} are constant, the boom sweep angle remains constant, the keel and booms do not deflect under load, and the drag of the fuselage acts through the vehicle center of gravity.

Taking moments about the vehicle center of gravity and using the geometry shown in figure 15 yields the following relationship

$$C_m = \left(\frac{x - x_0}{l_k}\right) C_{N_w} + \left(\frac{z - z_0}{l_k}\right) C_{X_w} \tag{2}$$

where

$$x_0 = 0.46 l_k$$

$$z_0 = 0.08 l_k$$

By letting $C_m = 0$ in equation (2), the locus of the center-of-gravity positions for constant trimmed lift coefficient in relation to the wing can be determined. These loci are shown in figure 16.

Differentiating equation (2) with respect to angle of attack yields the following relationship

$$C_{m_\alpha} = \left(\frac{x - x_0}{l_k}\right) C_{N_{\alpha_w}} + \left(\frac{z - z_0}{l_k}\right) C_{X_{\alpha_w}} \tag{3}$$

where (ref. 2)

$$C_{N_{\alpha_w}} = 0.0432 \text{ per deg}$$

$$C_{X_{\alpha_w}} = -0.02 \text{ per deg}$$

From this relationship, the locus of center-of-gravity positions for constant C_{m_α} in relation to the wing can be determined, as shown in figure 16.

To achieve an adequate airspeed range, it was desired to trim the test vehicles from a lift coefficient of 0.180 to 1.1 with sufficient longitudinal

stability over this range. As shown in figure 16, C_{m_α} becomes less negative as the center of gravity is moved closer to the keel. To provide adequate C_{m_α}, the center of gravity was located 48 percent of the keel length below the keel. The forward and rearward center-of-gravity travel shown resulted from the requirement to trim over a wide range of lift coefficients.

REFERENCES

1. Rogallo, Francis M., Lowry, John G., Croom, Delwin R., and Taylor, Robert T.: Preliminary Investigation of a Paraglider. NASA TN D-443, 1960.

2. Hewes, Donald E.: Free-Flight Investigation of Radio-Controlled Models With Parawings. NASA TN D-927, 1961.

3. Anon.: Flexible-Wing Manned Test Vehicle. Rep. 61B131A (Project 9R 38-01-017-72, Contract DA 44-177-TC-721), Ryan Aero. Co. (San Diego, Calif.), June 25, 1962.

4. Hoerner, Sighard F.: Fluid-Dynamic Drag. Pub. by the author (148 Busteed, Midland Park, N. J.), 1958.

TABLE I.- PHYSICAL CHARACTERISTICS OF THE TEST VEHICLES

	Vehicle A	Vehicle B
Weight (including pilot), lb	530	640
Parawing:		
Area (total cloth), sq ft	150	150
Loading, lb/sq ft	3.54	4.27
Keel chord, ft	14.7	14.7
Boom length, ft	14.7	14.7
Boom diameter, percent keel length	1.4	1.4
Sweepback angle (booms), deg	50	50
Attachment point, percent keel length	47.5	47.5
Vertical distance from attachment point to center of gravity, percent keel length	48	47.6
Boltrope, percent	0	Variable
Fuselage, ft:		
Length	9.42	9.42
Height	11.16	11.16
Width	6.75	6.75
Control system:		
Longitudinal -		
Change in wing incidence, deg	0 to 22	0 to 22
Change in wing incidence per stick travel, deg/in.	1.13	1.13
Lateral -		
Change in wing angle relative to fuselage, deg	±14	±7.5
Change in wing angle per stick travel, deg/in.	0.95	0.42

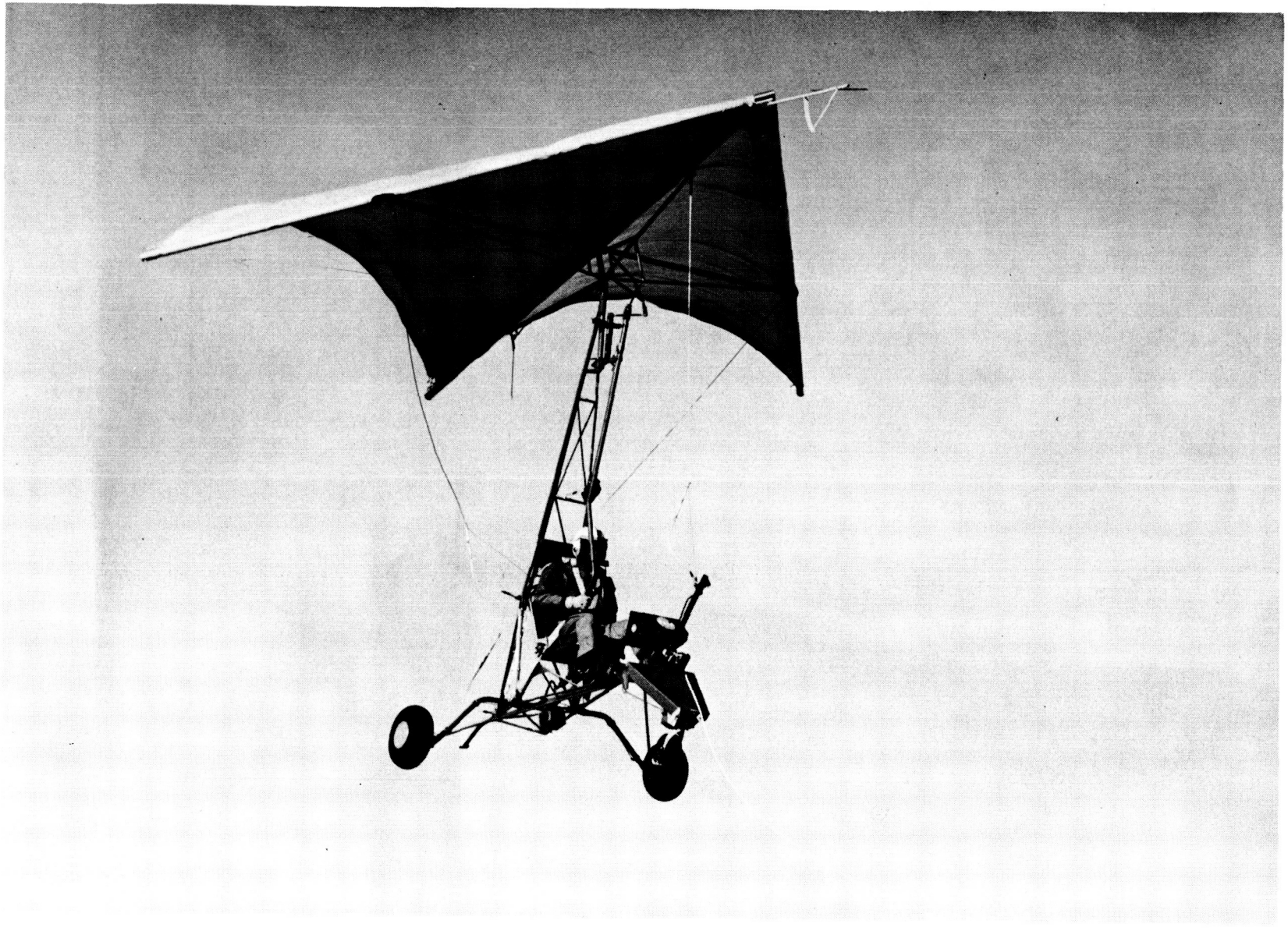

Figure 1.- Vehicle A in flight.

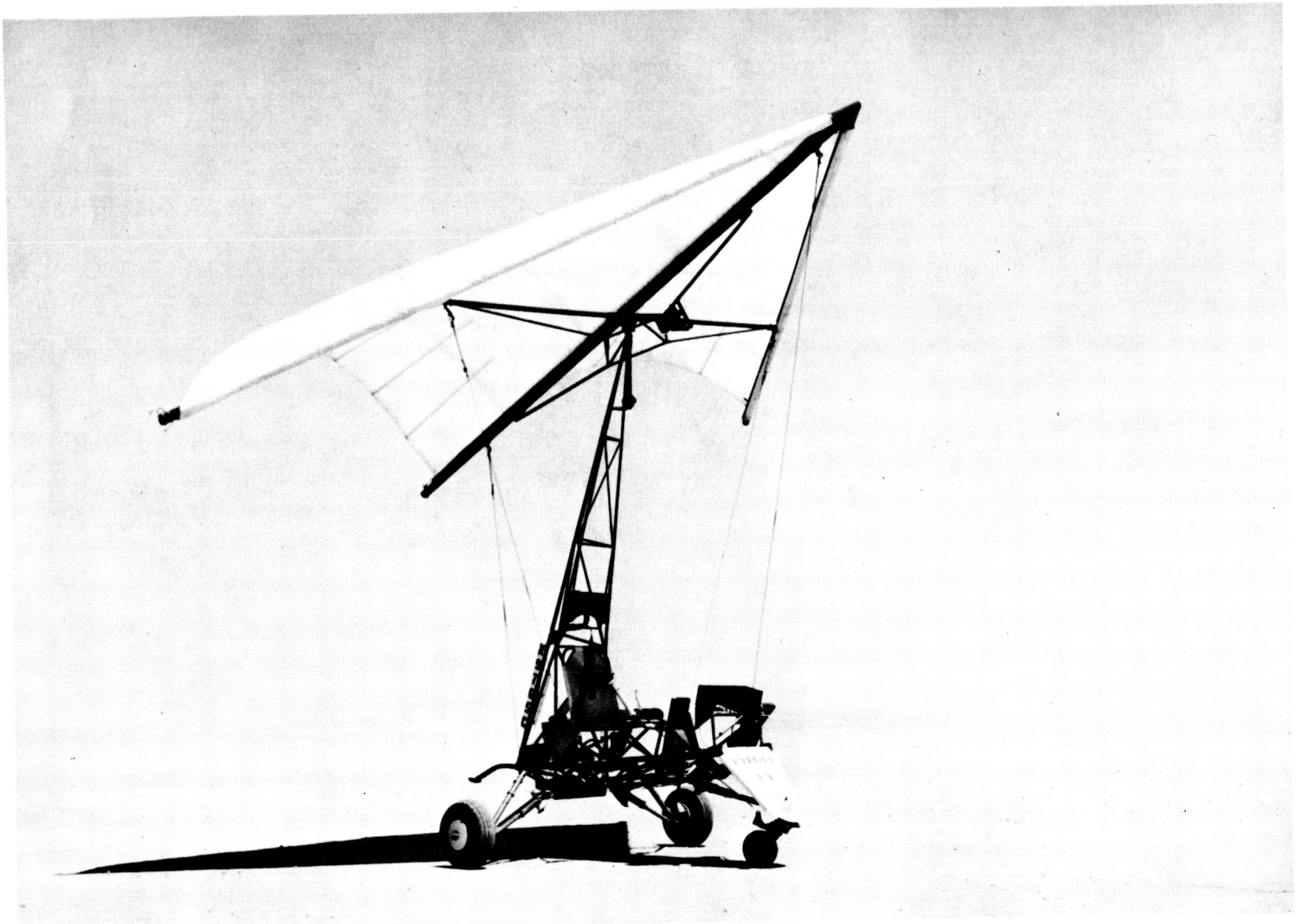

Figure 2.- Vehicle B.

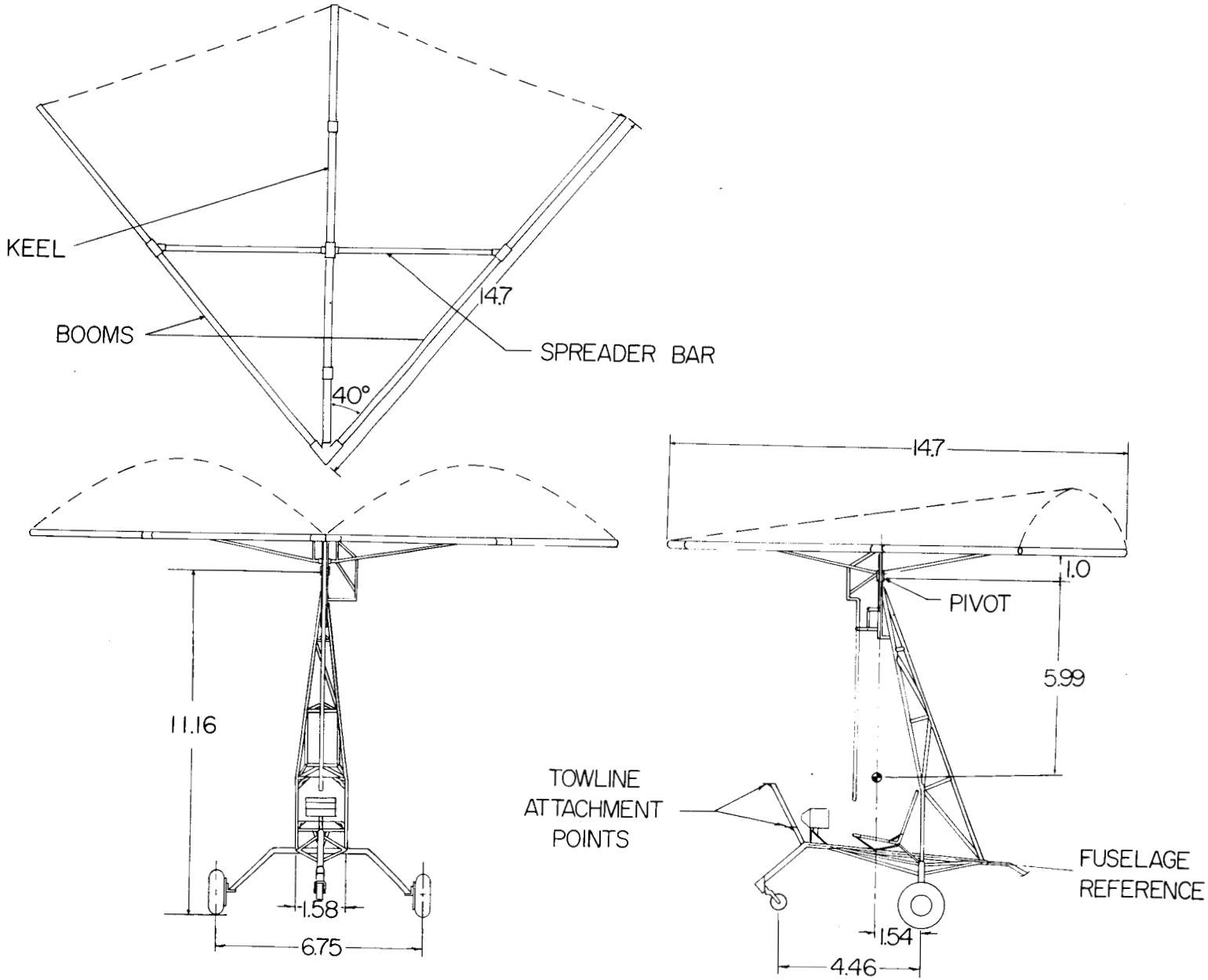

Figure 3.- Three-view drawing of vehicle A. All dimensions in feet unless otherwise noted.

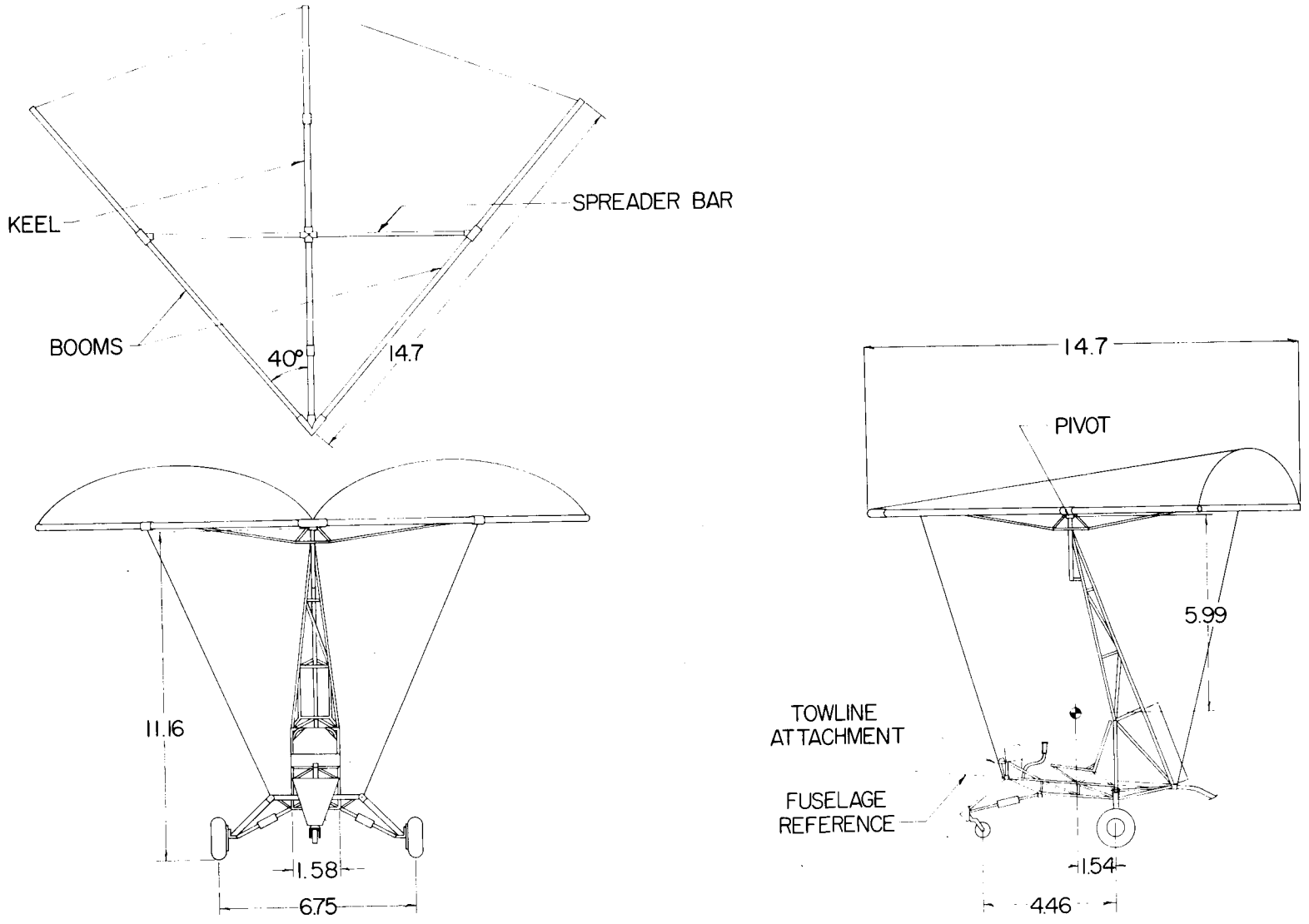

Figure 4.- Three-view drawing of vehicle B. All dimensions in feet unless otherwise noted.

Figure 5.- Photograph of control linkage used on vehicle A.

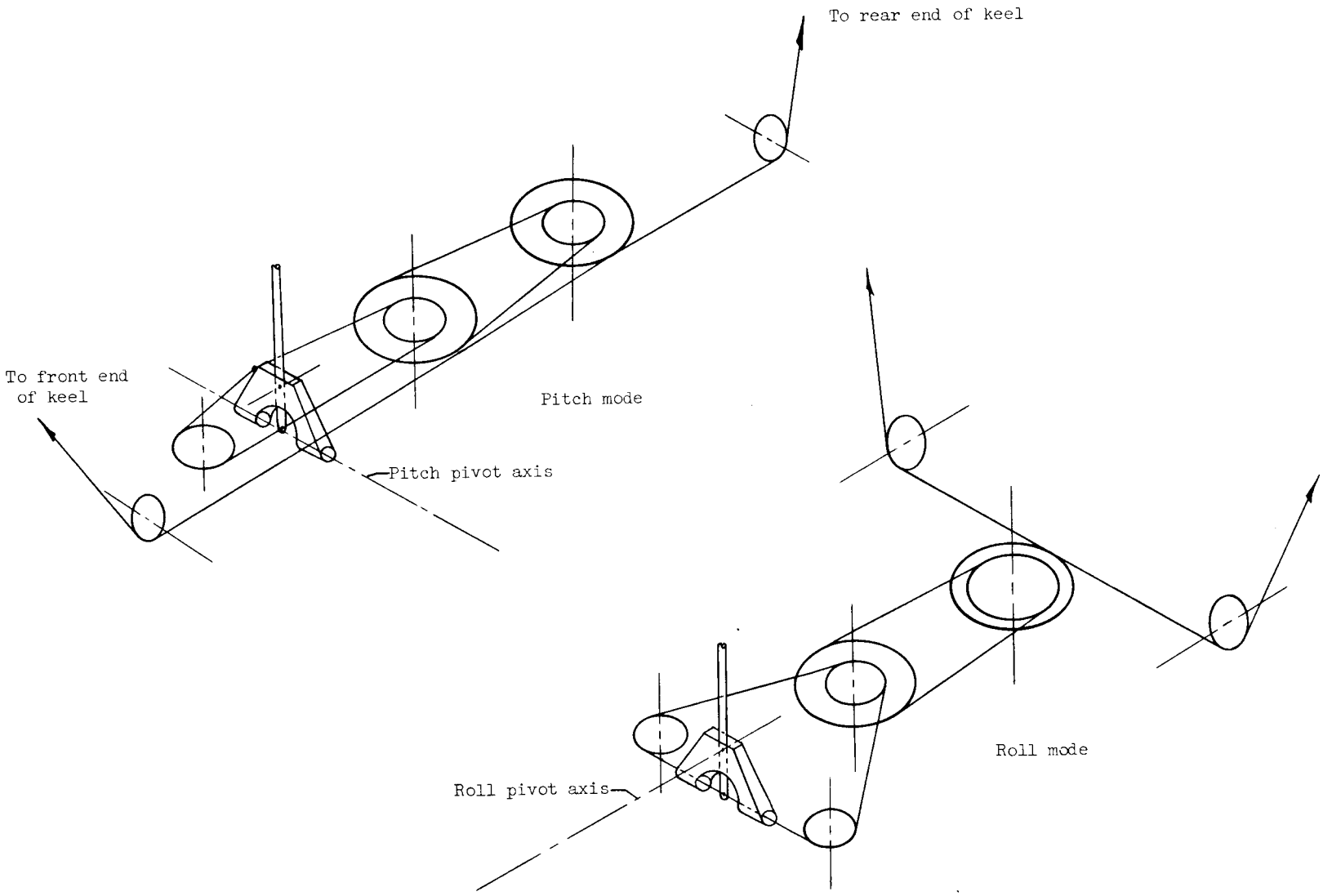

Figure 6.- Schematic drawing of control system used on vehicle B.

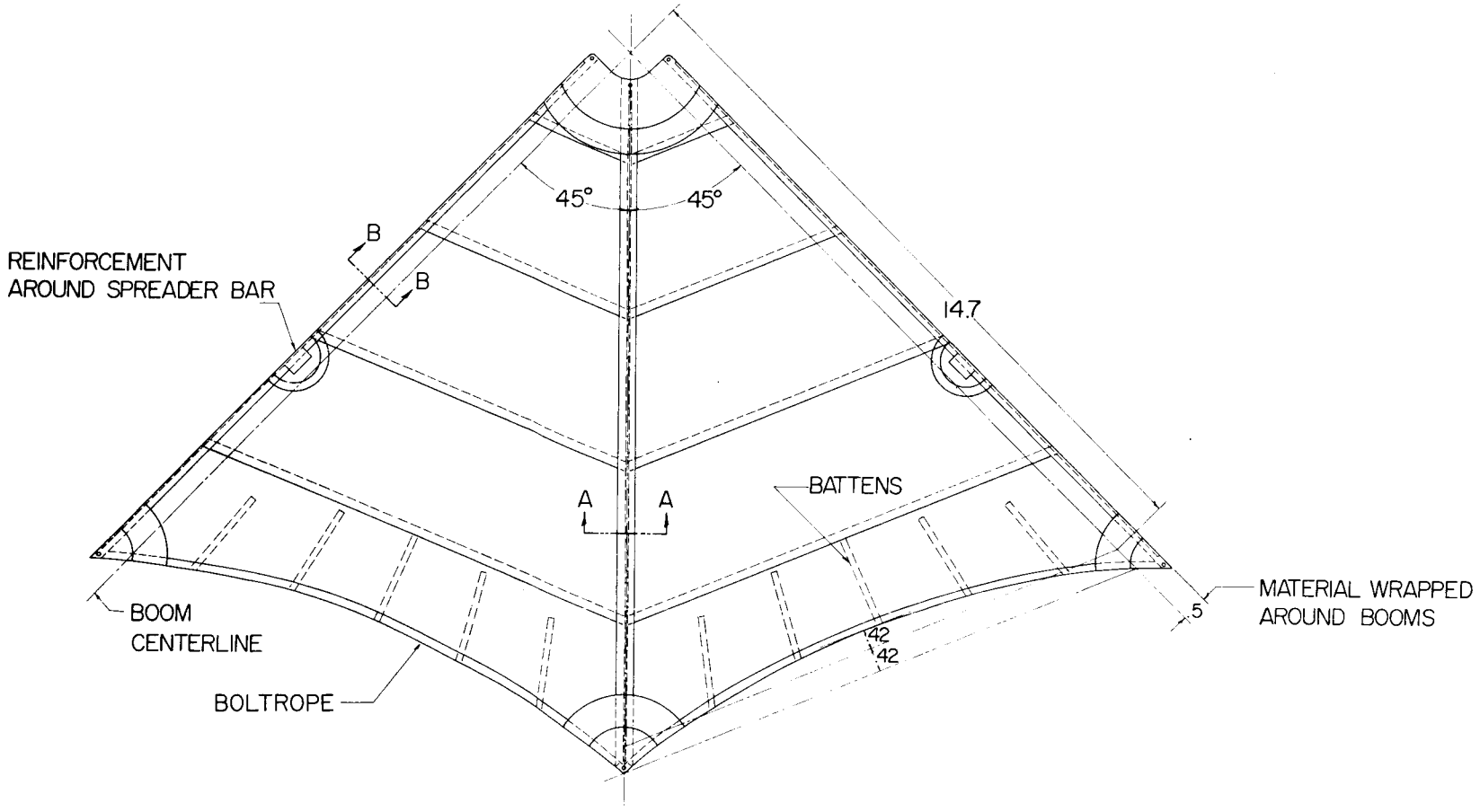

Figure 7.- Drawing of wing flat pattern showing details of membrane used on vehicle B. All dimensions in feet unless otherwise noted.

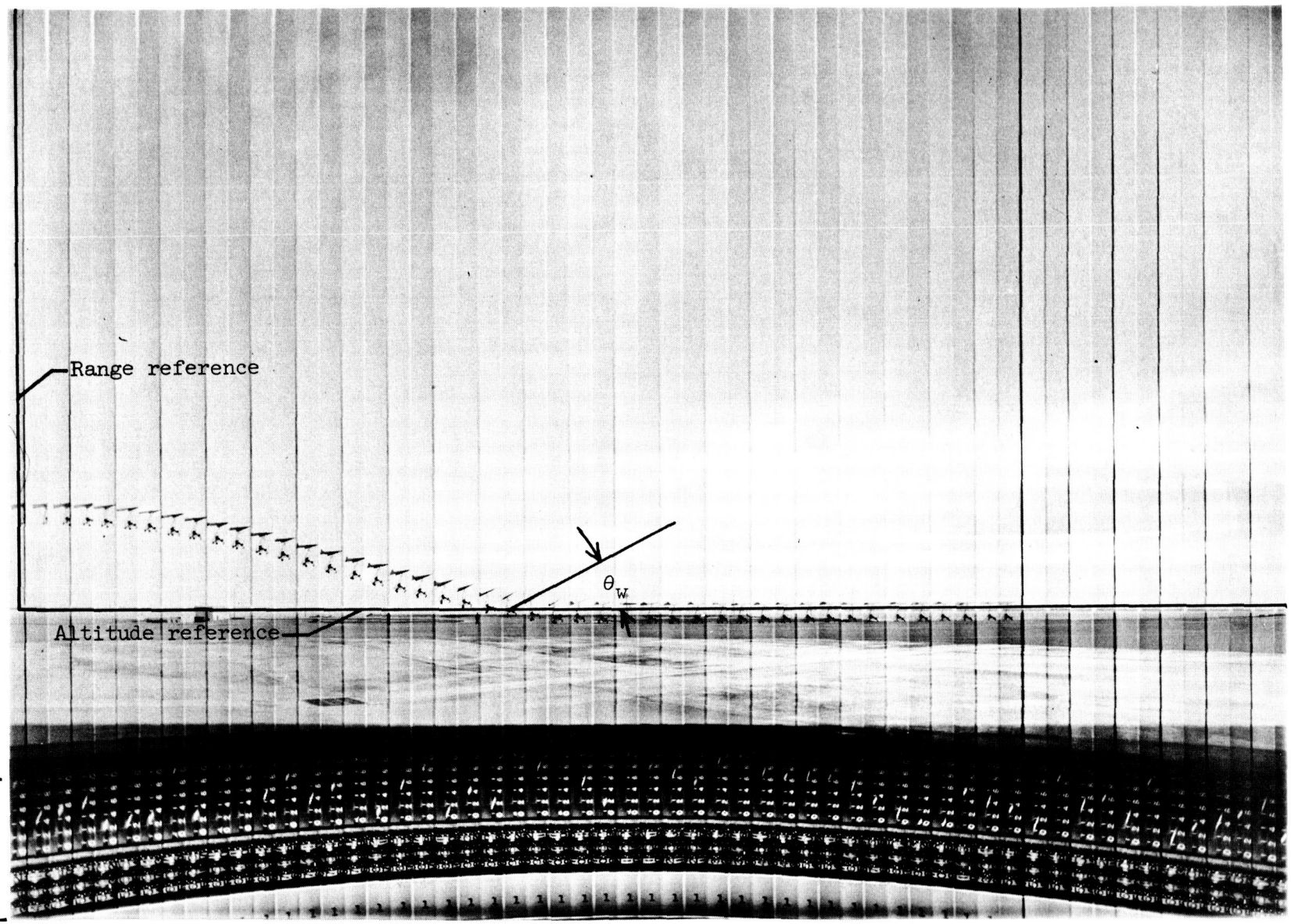

Figure 8.- Typical Fairchild photograph of vehicle A free flight.

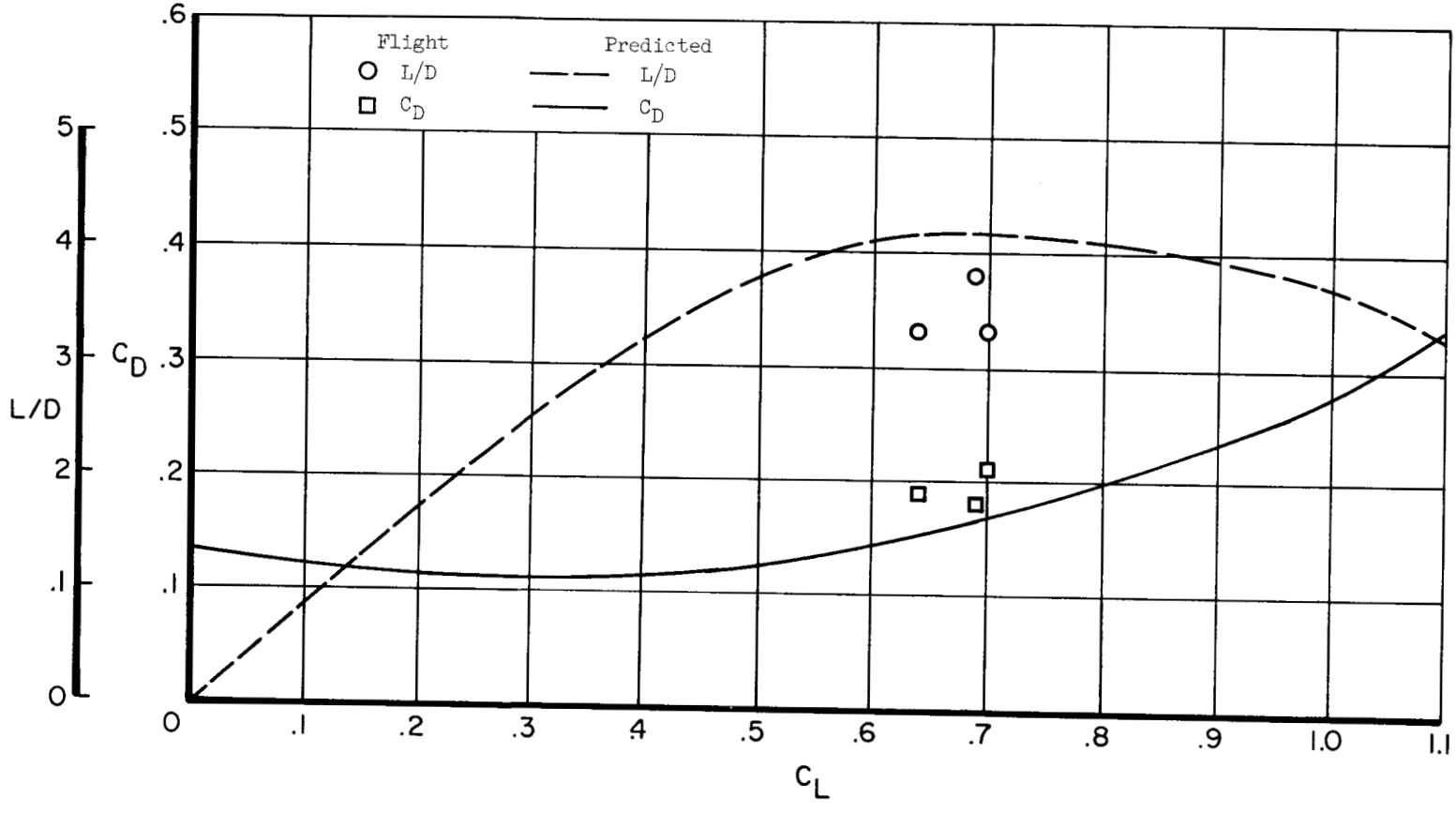

Figure 9.- Variation of drag coefficient and lift-drag ratio with lift coefficient. Vehicle A.

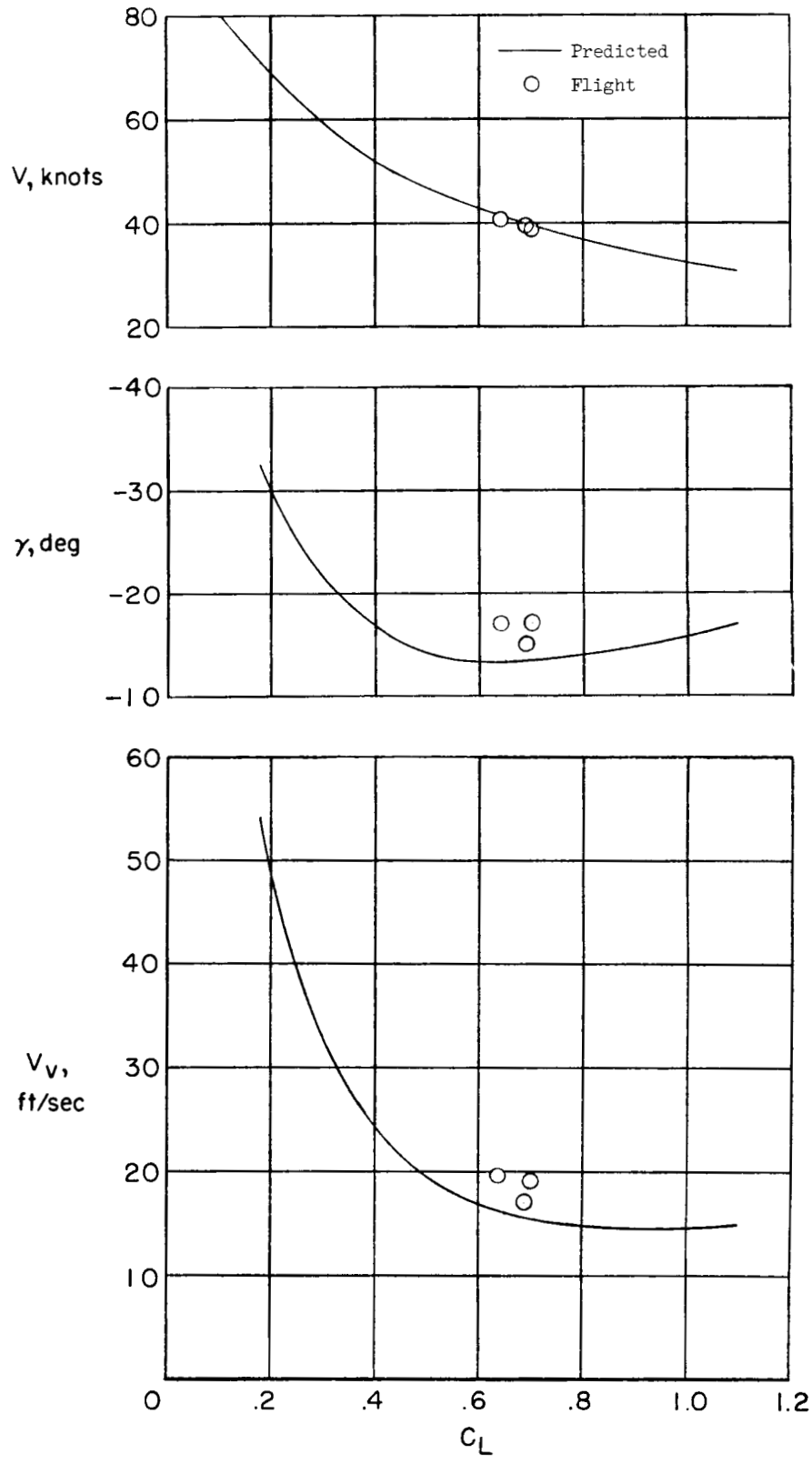

Figure 10.- Steady-state flight parameters as a function of lift coefficient. Vehicle A.

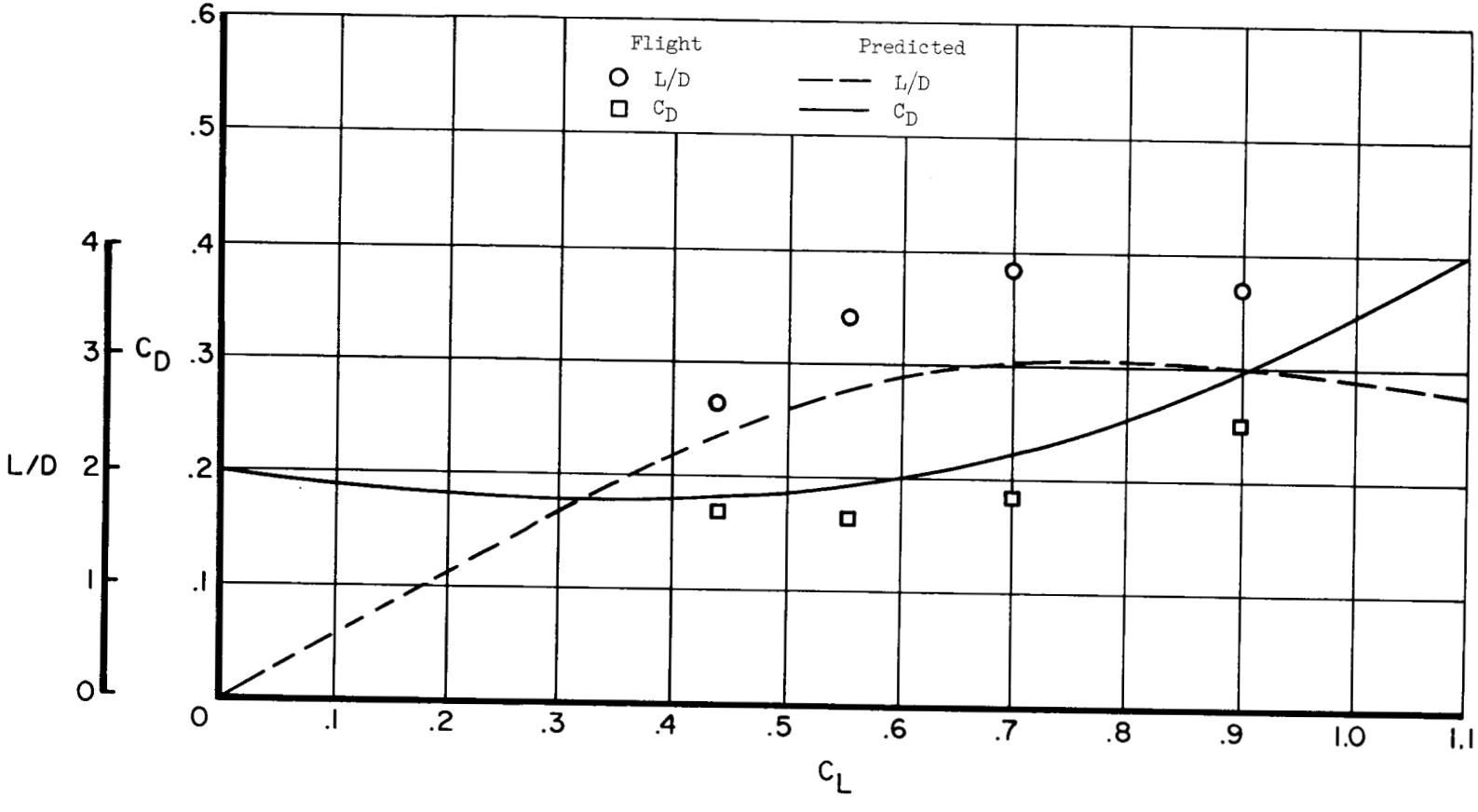

Figure 11.- Variation of drag coefficient and lift-drag ratio with lift coefficient. Vehicle B.

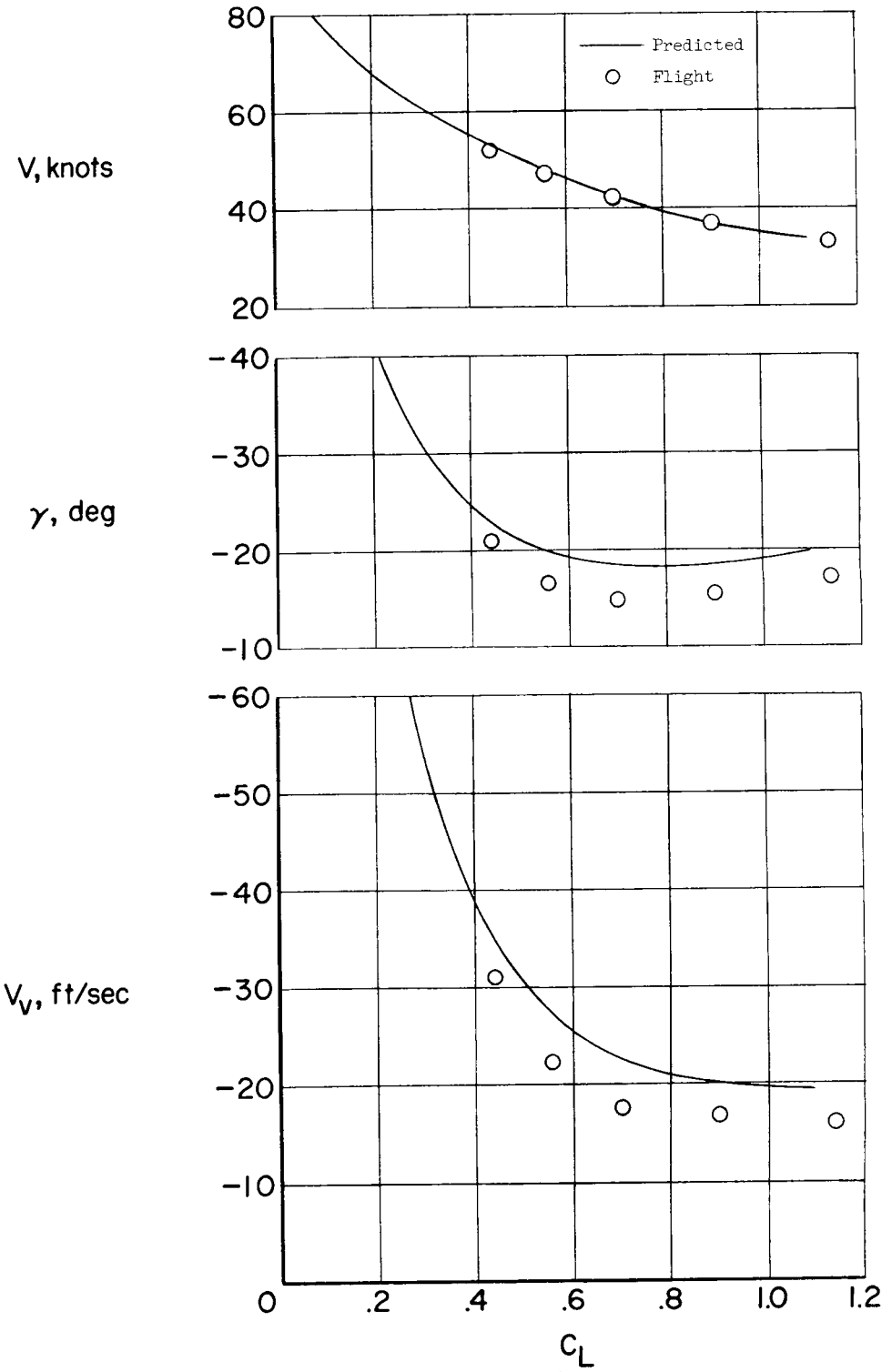

Figure 12.- Steady-state flight parameters as a function of lift coefficient. Vehicle B.

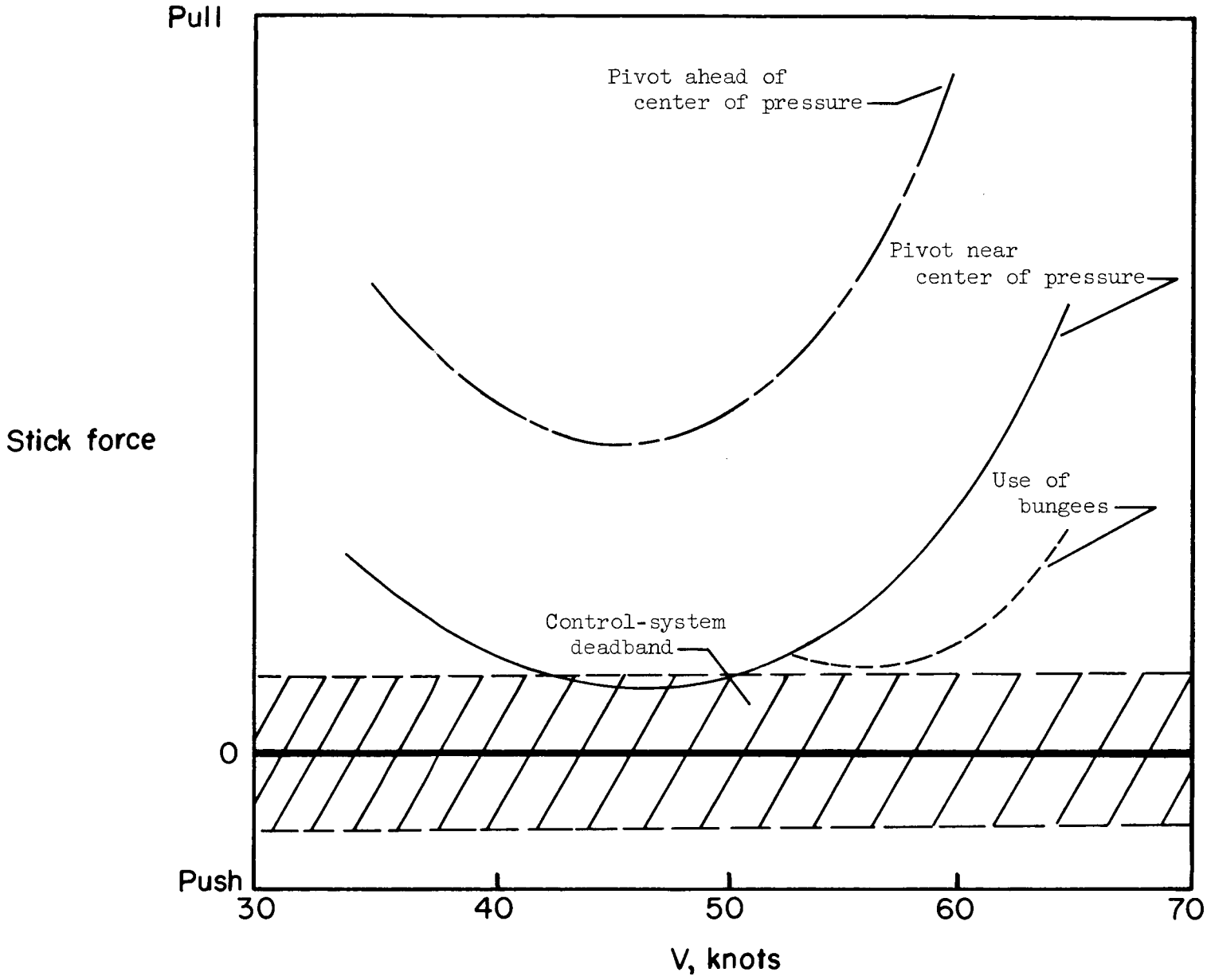

Figure 13.- Longitudinal stick forces for 1 g flight.

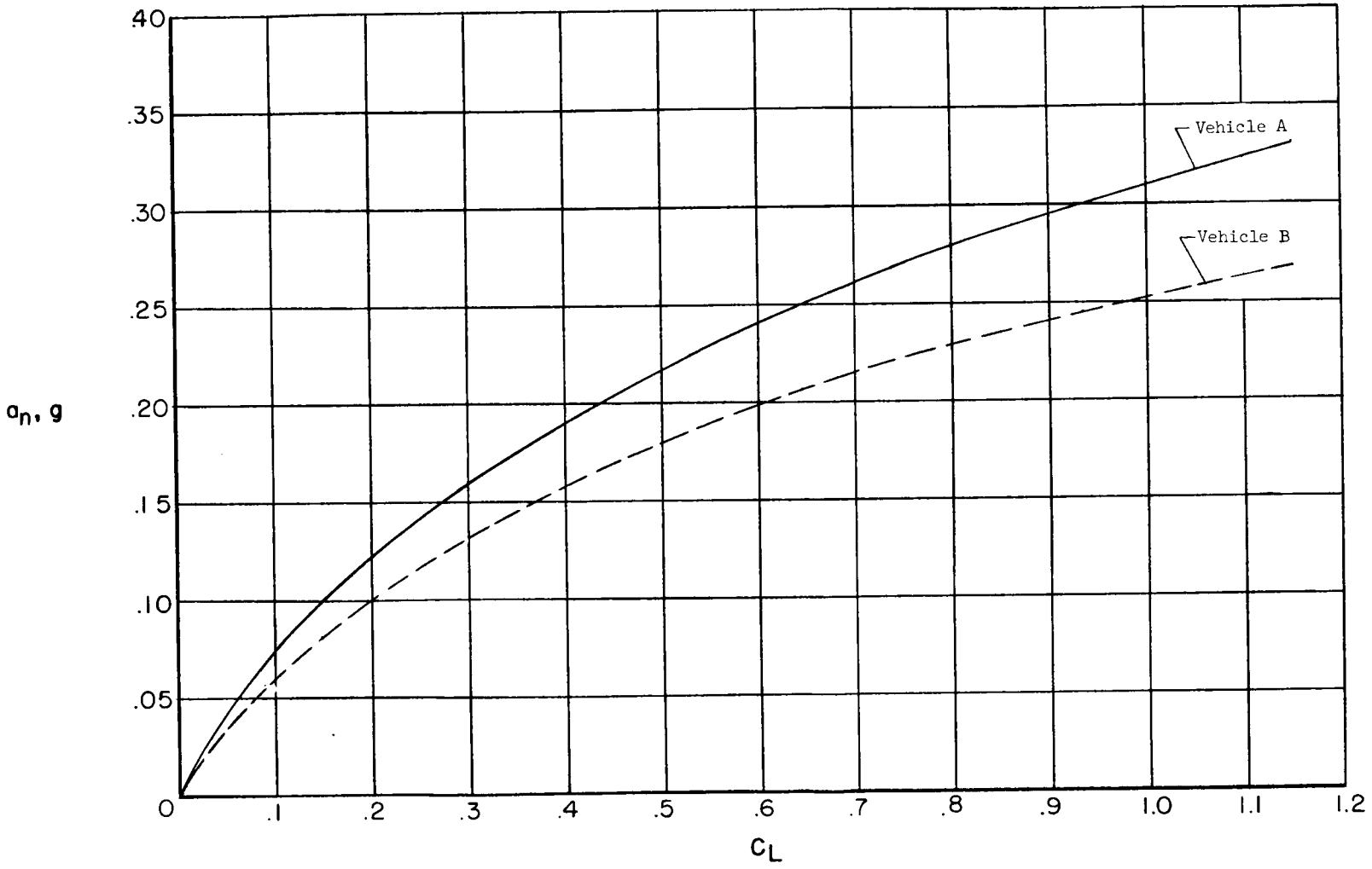

Figure 14.- Initial normal acceleration resulting from a 5-knot gust. Vehicles A and B.

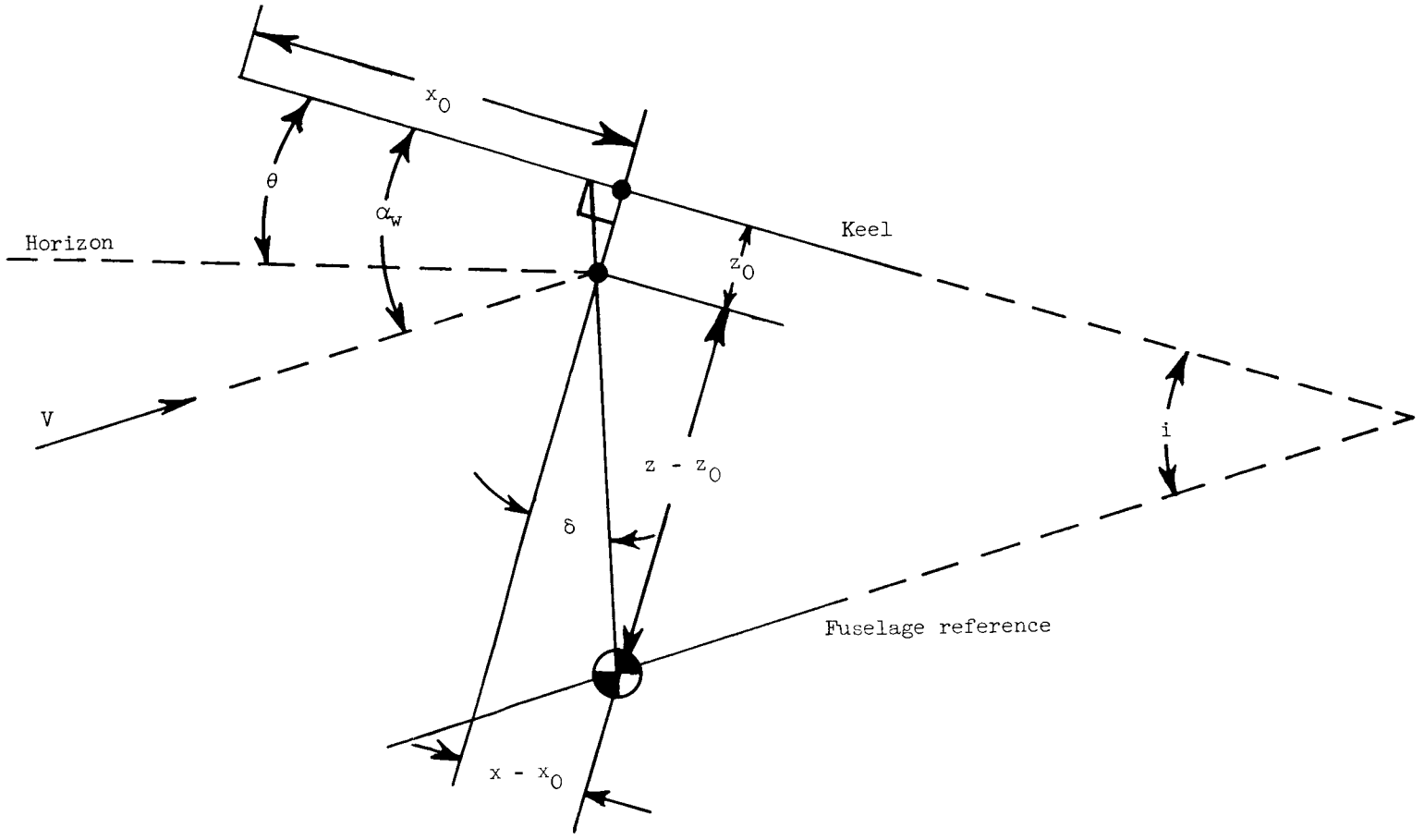

Figure 15.- Diagram of paraglider control geometry.

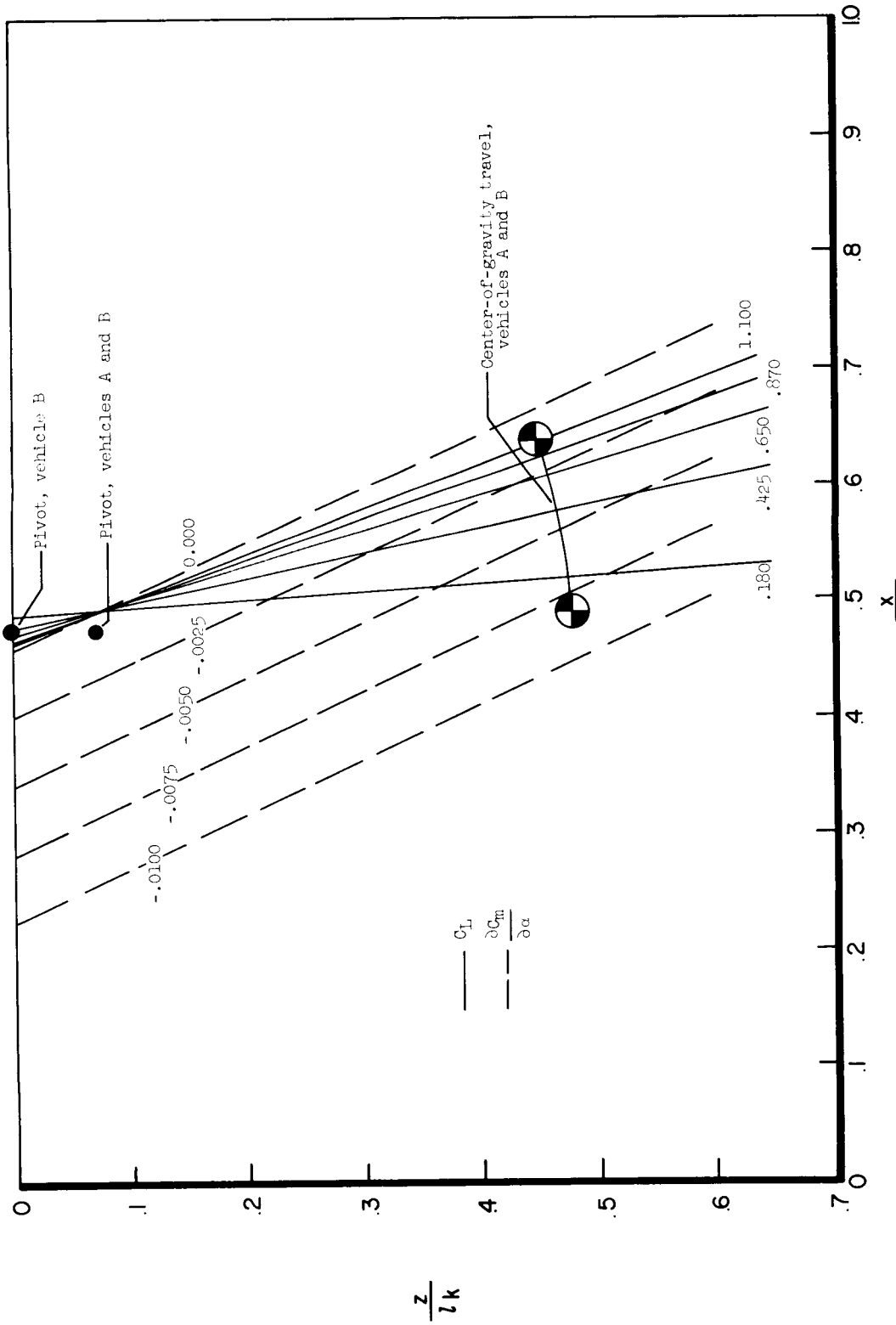

Figure 16.- Constant trim lift coefficient and longitudinal stability. Vehicles A and B.